SOUTHEASTERN GEOLOGY
V. 47, No.1, February 2010, p. 15-26

NATURAL OCCURRENCE OF ELEVATED ARSENIC AND SELENIUM IN GEORGIA REGOLITH: IMPLICATIONS FOR THEIR RELATIVE MOBILITY IN PIEDMONT SOILS

PAUL A. SCHROEDER

Department of Geology
University of Georgia
Athens, Georgia 30602-2501

ABSTRACT

Arsenic concentrations of >100 ppm were detected above the regional value of ~7 ppm in soils near the Georgia Brevard Zone using optical emission spectroscopy (OES). Natural, anthropogenic, and false-positive hypotheses were tested to determine a most likely explanation. Induction coupled plasma mass spectroscopy (ICP-MS), X-ray diffraction, optical microscopy, electron microprobe analysis, and historical aerial photographs were subsequently used to determine the most parsimonious hypothesis. ICP-MS results indicated positive detection and verified accuracy of the OES-measured As and concentrations of many other trace elements such as Se. Arsenopyrite is the primary As- and Se-bearing phase in the underlying mafic schist bedrock. The associated bedrock mineral assemblage suggests a fossil hydrothermal system protolith and subsequent prograde and retrograde moderate metamorphism. As/Se ratios in the 20m-thick saprolite are much higher (~2000) than regional baseline values for the SE United States (~15) and the underlying bedrock itself (~45). The high soil-saprolite As/Se ratio empirically supports a theoretical ionic potential basis for greater solubility and transport of Se (relative to As) out of the weathered zone and into rivers. Published As/Se ratios for biomonitor proxies living in rivers that drain through the Brevard Zone (~0.6) further support the idea that As in saprolites of the Piedmont in the SE United States is more conservative in fate and transport than Se.

INTRODUCTION

Arsenic (As) and selenium (Se) in soils of the southeastern United States (SE U.S.) have been generally mapped or delineated by low-density and shallow depth (<20 cm) soil sampling surveys of areas relatively unaffected by human activities (Shacklette and Boerngen, 1984) or by site-specific surveys of areas known to be significantly impacted by human activities (Kukier and others, 2001; Jackson, 1998). Canonical baseline values for As and Se in conterminous eastern U.S. surface soils are reported to be about 7 and 0.5 parts-per-million (ppm), respectively, resulting in an As/Se ratio of about 15 (Shacklette and Boerngen, 1984). Numerous international and national regulations and guidelines for As and Se exposure exist for air, water, and food because they are considered to cause adverse health effects when absorbed in high concentrations (Frankenberger, 2002). Examples of exposure limits include (1) the U.S. Environmental Protection Agency (EPA) recommendation of a maximum As contamination limit of 0.010 ppm for drinking water, (2) the U.S. Occupational Safety and Health Organization (OSHA) recommendation of a permissible As exposure limit of 0.01 mg/m^3 over an eight hour period, and (3) the U.S. Food and Drug Administration stipulation of As limits at 0.5 to 2.0 ppm for certain animal by-products treated with As-bearing drugs (Anonymous ATSDR report, 2006). The Georgia Environmental Protection Division (EPD) notes that releases resulting in As and Se concentrations in excess of 41 and 36 ppm, respectively requires notification (Georgia State rule 391-3-19-04). Concentrations of As and Se in soils are not specifically regulated by these guidelines, but are factored into the assessment of EPA's Na-

Figure 1. Location map (inset) and aerial photographs of study site. Left image is 1938 photo showing primary land use as forested with remnants of agricultural tilling. Right photo shows 2007 use as mixed residential and industrial parks. Bold dark line in NW corner of right photo delineates SE extent of the Brevard Zone. Lines on right photo delineate formation contacts as published by (Dicken, 2005). All rocks are Precambrian-Cambrian with lithology noted by following symbols: fg2 -Biotitic Gneiss Undifferentiated; gg1 - Granitic Gneiss; pms7 - Button Mica Schist undifferentiated; fg3 - Biotitic Gneiss/Mica Schist/ Amphibolite; pm2 - Metagraywacke/ Mica Schist. Sample location is at 33° 55′ 43.40″ N, 84° 15′ 34.75″ W. Right photo modified from Google Earth © Tele Atlas.

tional Priorities List promulgated by the 1980 U.S. Comprehensive Environmental Response, Compensation, and Liability Act (CERCLA). As part of due diligence associated with performing CERCLA-prompted Phase I and II environmental site assessments (standardized by EPA), soil As and Se concentrations in excess of regional background levels appear to be the threshold to report a potential for threat to human health and/or the environment. Georgia EPD release thresholds for reporting As and Se are about 6 and 72 times regional baseline values, respectively.

As and Se concentrations observed in excess of the regional background can be attributed to multiple factors. Anthropogenic factors and natural factors are the two main categories for explaining or finding elevated levels in soils. Human activities such as pesticide application, wood preservative production, coal fly ash production, and acid-sulfide mine tailing accumulations account for the major sources of anthropogenic As and Se contaminant sites in the SE United States (Frankenberger, 2002). The purpose of this study is to document a natural occurrence of elevated As and Se concentrations in soils and to provide empirical insights into their relative fate and transport in the near surface weathering environment of the Piedmont SE United States.

BACKGROUND

The study site is located in the Piedmont of Georgia, Gwinnett County (Figure 1 inset) and was initially identified in response to reconnaissance work associated with a phase 1 assessment, in which As-bearing soils were noted in surface auger samples tested by optical emission spectroscopy (OES) (see more detailed comments below in methods selection). Causes for elevated As concentrations in the soil were considered with multiple working hypotheses, which included (1) a human source or (2) a nat-

ural source, or (3) false positive results. Common anthropogenic sources of As in the Georgia Piedmont include pesticide applications associated with control of the cotton boll weevil around the 1920's (Williams and others, 2005; Haney and others, 2009) and herbicide control for cotton growing, which occurred into the 1990's (Bednar and others, 2002). Historical aerial photography of the study site indicates it was utilized for agricultural purposes as far back as the 1930's, as evidenced by the plowing contours seen in Figure 1 (approximate center of left photo). The area has since rapidly developed into industrial parks and is now proximal to residential areas and major rail and road transportation lines (Figure 1, approximate center of right photo). Arsenopyrite has been reported in association with gold mining and tailings (EPA Report, 2003), the latter of which has been known to occur in north Georgia. If such tailings were transported to the site and dumped, then this represents a possible As and Se source.

Quadrangle-scale geologic mapping for this area indicates the study site is situated on lower Paleozoic metamorphic rocks with SW-NE trending structures (Higgins, 1968). These rocks have experienced numerous cycles of intrusion, folding, faulting, and deformation with the most recent influences of metamorphism associated with final stage collisions of Eurasian and North American Plates (200 to 230 Ma) and subsequent mafic dike emplacement related to cratonic rifting. Figure 1 shows approximate locations of formation contacts in the study area, as well as the trace of the Brevard Zone. The Brevard Zone is a narrow SW-NE trending feature with numerous interpretations and likely owes its origins to multiple mechanisms of thrust faulting, strike-slip faulting, overturned folding, and the development of complex features associated with prograde and retrograde metamorphism (Crawford and Kath, 2001). The study site (Figure 1) is mapped as "Button schist", a term noted by Higgins (1966) for the pattern of two distinct subparallel cleavages that appear upon weathering. These rocks occur throughout the Brevard Zone and are described as having crystalline texture resulting from metamorphic recrystallization under conditions of high viscosity, directed pressure, and some recrystallized after granulation (Reed, 1970).

METHODS

Impetus for study was based on prior surface sampling of soils (<5 m) and using OES analysis via EPA method 6010C (Jones and others, 1987; Hassan and Loux, 1990), with some As concentrations reported above the regional baseline value of ~7 ppm. Reported OES-determined As concentrations ranged from 4 to 375 ppm. A two-point drilling program was conducted to continuously core from the surface through the saprolite and into the rock basement. Two hand-auger samples from approximately the same locations were also taken to a depth of approximately 1.5 m below the surface. The auger samples were immediately tested using Induction Coupled Plasma Mass Spectrometry (ICP-MS) because of the potential for false positive As testing by ICP-OES in the presence of Al-rich materials (Jones and others, 1987) and because the regional bedrock and soils are known to be aluminous (Higgins, 1966). ICP-MS technology is capable of simultaneous determination of up to 80 elements in a liquid sample in a single run of a few minutes. The mass-selective detector is extremely sensitive, particularly for heavier elements, giving very low, down to parts per trillion, detection limits. The detector system is also relatively immune to many of the chemical and spectroscopic interferences that plague ICP-OES systems (Hassan and Loux, 1990). Seventy-three elements were determined on individually extracted samples using a proprietary Perkin-Elmer Elan 6000 ICP-MS semi-quantitative element scan called "Total scanQuant." The instrument was also calibrated for As, Se and several other metals of environmental interest (including EPA regulated metals) and run using a proprietary calibrated technique called "fullQuant".

Cores were sampled approximately every meter (Table 1) and hand ground for ICP-MS and X-ray diffraction powder analysis (XRD) using a zirconium mortar and pestle with alcohol as a grinding agent. For soils, sediments,

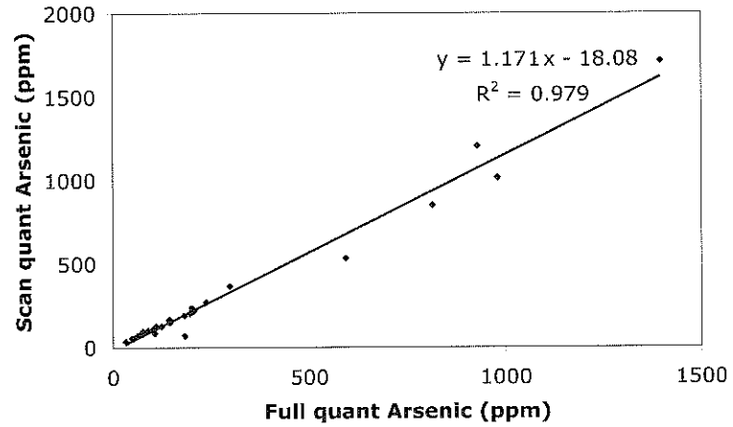

Figure 2. Quantitative analysis of As concentration in cores #1 and #2 sampled in Gwinnett County, GA. Axes depict duplicate analyses using two different proprietary quantification schemes. Line represents least-squares minimization fit to the data assuming a linear model. Cross plot using Se values produces similar coefficients.

rocks and organics, a boiling nitric acid digest was used to extract metals (EPA method 3050A). This involves digestion of the sample in concentrated nitric acid on a hot plate, followed by hydrogen peroxide to further oxidize organics and solubilize metals (Edgell, 1988). This works less well for soils and rock material and very well for highly organic samples (e.g., plant tissue). The concentrations reported herein therefore, may reflect slightly varied values relative to the total mass of the soil or rock because less soluble silica and aluminum oxide phases may not be totally dissolved. The hand auger near-surface soil samples measured by ICP-MS showed similar arsenic values to those measured by ICP-OES. It was therefore concluded that the measured arsenic concentrations using ICP-OES are accurate and grounds for nullifying the false positive hypothesis is justified.

The powdered bedrock material for XRD analysis was transferred to 30 x 30 mm mount and pressed to minimize transparency and preferred orientation. Data were collected using a Scintag diffractometer, with Co Kα radiation, a 250 mm goniometer circle, 2°/4° primary and scattering slits, 0.5°/0.3° scattering and receiving slits, 40 kV and 35 mA, a step size of 0.01°, and a scan rate of 2° per minute. Selected pieces of the bedrock schist from the unweathered portion of the core were cut, polished, and prepared for electron microprobe analysis (EMPA) using wavelength dispersive spectroscopy (WDS) and backscatter secondary electron imaging (BSE). A representative thick section was cut perpendicular to foliation and fractures in the schist. The polished mount was carbon coated for EMPA-WDS using a JEOL JXA-8600 Superprobe. Beam current was 15 nA and accelerating voltage was 15 keV. Grains were analyzed for Fe, As, and, Se using natural and synthetic mineral standards.

RESULTS

Coring resulted in the retrieval of 23 and 25m of continuous sampling for cores #1 and #2, respectively (Table 1). Saprolite thicknesses for each core are approximately 20m and 22m, respectively and approximately 3m of solid bedrock core were recovered from each drill hole. Foliations of the core are oriented with a dip of about 25°, which is slightly less than the regional dips of 36°-40° SE, published by Higgins and Crawford (2007). Table 1 includes depths sampled for ICP-MS analysis, with the solid line indicating sampling above and below the bedrock-saprolite interface.

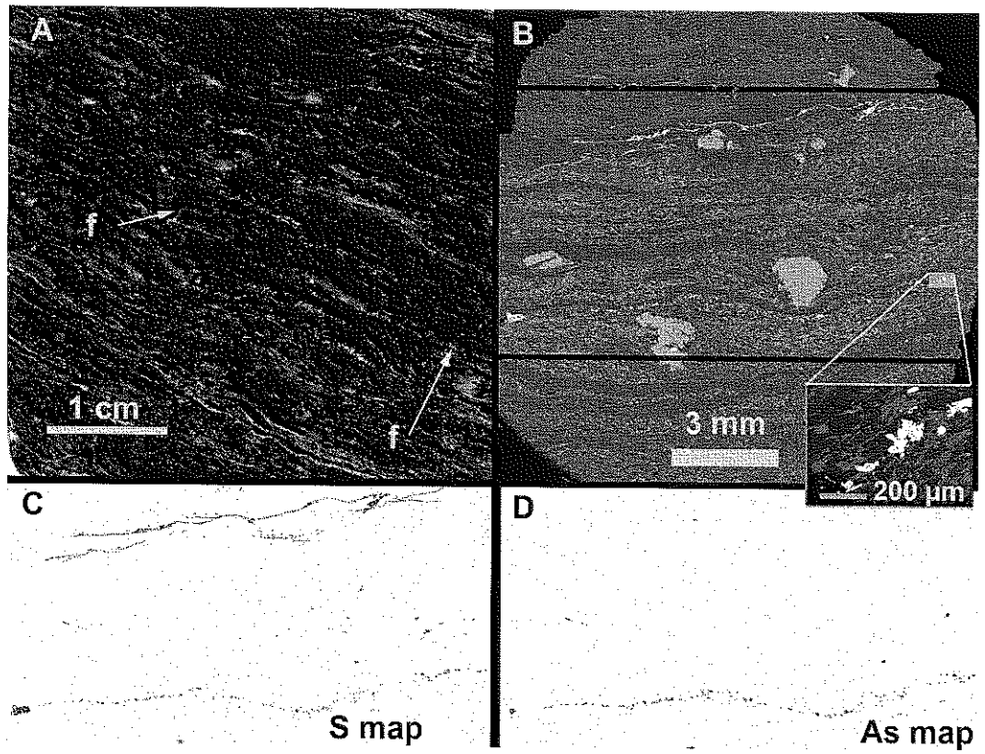

Figure 3. Micrographic images of schist from core #2 (depth 21.8 m). A) Reflective light image of polished core section cut perpendicular to dipping foliations. With exception to occasional cross-cutting brittle fractures (f), all primary mineral fabrics appear to follow the foliation, B) BSE image reveals electron dense (brighter) minerals following foliation trends. Horizontal lines depict mapped areas shown below. Inset shows higher magnification view of arsenopyrite grains. C) Sulfur WDS map of same area shown above in BSE. Two dark bands (one in the top and other in bottom) highlight concentrations of pyrite (top) and arsenopyrite (bottom), D) Arsenic WDS map of same area shown above in BSE, but only lower dark band highlights concentration of arsenopyrite. Note As blebs follow foliations, while S follows both blebs in foliations and pyrite in fractures.

ICP-MS duplicate analyses for As using the different quantitative approaches reveals values are reproducible over the range from 37 to 1710 ppm and having near unity correlation (Figure 2). A plot using Se scanQuant and fullQuant values (not shown) reveals linear trend coefficients similar to As, with the main difference being the concentration range, which varied from 0.03 to 6.12 ppm for Se. Semi-quantitative scanQuant ICP-MS results in Table 1 are reported to three significant figures. The focus of this study is the source and relative fate of As and Se, therefore discussion of other elemental trends is beyond the study scope, however data are provided for future workers.

XRD and optical analyses of the bedrock schist from the core hole bottom reveals a mafic minerals assemblage, with quartz, biotite, muscovite, garnet, clinochlore, albite, laumontite, and pyrite occurring as major phases (Figures 3 and 4). Foliation and fracture fabrics dominate the rock's texture. Included in the foliations are most all the above mineral grains, which appear to follow slight undulating mm-scale waves (Figures 3A and 3B). Cross-cutting brittle fractures comprises a fabric that is often filled with pyrite and laumontite. These fracture-fills clearly post-date the foliation and are indicative of retrograde metamorphism of a fossil hydrothermal system (Deer and others, 2004). Sulfur and

Table 1. ICP-MS FullQuant results for elemental concentrations using EPA extraction method 3010A. Concentrations are reported as ppm (mgkg).Solid line marks samples from above and below the saprolite/bedrock contact.

Core 1

Depth (m)	Sc	Ti	V	Cr	Mn	Fe	Co	Ni	Cu	Zn	Ga	Ge	As	Se	Br	Rb	Sr	Y	Zr	Nb	Mo	Pd	Ag	Cd	In	Sn	Sb
0.6	2.54	733	139	44.6	257	43200	13	27	22	115	15	0.14	70	0.92	0.52	119	4.5	43.9	14.6	0.07	0.19	0.03	0.02	0.04	0.08	1.05	0.01
1.8	1.35	555	102	42.4	732	48244	12	24	102	50	12	0.13	237	0.82	0.38	125	2.3	32.2	22.3	0.08	0.00	0.89	0.04	0.07	0.05	0.37	0.01
3.1	1.13	470	79	38.4	669	42964	23	26	49	68	10	0.12	163	0.61	0.27	84	3.0	21.3	15.9	0.07	0.14	0.01	0.03	0.07	0.04	0.45	0.00
4.3	2.50	648	155	50.5	1446	45588	29	39	20	123	15	0.15	130	0.68	0.94	106	4.7	32.1	16.7	0.05	0.00	0.04	0.05	0.14	0.07	0.19	0.01
5.8	2.68	732	122	62.8	334	39349	12	31	5	145	15	0.12	56	0.58	0.82	123	4.7	20.1	14.2	0.05	0.14	0.03	0.02	0.05	0.07	0.22	0.00
7.6	0.30	234	37	20.5	67	26473	5	9	44	40	4	0.07	97	0.51	0.46	196	3.3	14.0	12.6	0.11	0.38	0.01	0.02	0.08	0.01	0.11	0.00
8.5	0.81	534	66	30.4	298	36390	11	24	45	91	9	0.06	103	0.30	0.37	81	7.7	10.6	19.6	0.11	0.22	0.71	0.04	0.15	0.03	0.23	0.00
10.1	0.82	509	86	40.1	424	46291	18	35	38	39	9	0.07	162	0.42	0.44	103	7.3	11.6	14.2	0.12	0.19	0.44	0.06	0.23	0.03	0.23	0.01
11.6	1.97	746	158	32.0	666	45844	24	20	111	149	13	0.11	110	0.40	0.48	109	9.4	11.6	11.6	0.06	0.35	0.49	0.08	0.17	0.07	0.40	0.00
13.7	2.20	482	164	40.4	1057	72604	22	34	64	180	13	0.25	271	0.94	0.49	84	10.3	31.3	11.3	0.05	0.61	0.40	0.13	0.99	0.06	0.15	0.02
15.3	1.20	546	118	47.8	282	48175	25	29	53	61	10	0.10	218	0.54	0.31	97	10.1	17.4	9.9	0.09	0.65	0.03	0.07	0.27	0.04	0.38	0.01
19.2	0.77	412	88	39.7	86	33720	21	37	48	26	7	0.07	534	0.79	0.46	82	4.6	13.4	5.8	0.10	1.48	0.25	0.14	0.06	0.03	0.46	0.02
20.7	1.07	509	95	53.7	62	36521	31	41	68	38	10	0.04	1203	0.73	0.71	97	2.8	6.2	8.6	0.16	0.91	0.01	0.28	0.10	0.04	0.65	0.05
21.4	0.30	143	29	40.0	81	245774	20	177	132	70	7	0.14	86	3.13	0.84	9	44.0	13.6	11.6	0.21	1.16	0.10	0.24	1.73	0.04	0.83	0.87
21.8	0.80	69	9	8.5	18	37004	20	99	6	16	23	1.39	37	6.16	2.30	3	242.0	383.7	4.1	0.01	0.48	0.08	0.12	0.08	0.01	0.05	0.12

Core 2

Depth (m)	Sc	Ti	V	Cr	Mn	Fe	Co	Ni	Cu	Zn	Ga	Ge	As	Se	Br	Rb	Sr	Y	Zr	Nb	Mo	Pd	Ag	Cd	In	Sn	Sb
0.6	1.64	415	118	45.1	206	48436	15	35	85	50	12	0.08	86	0.79	0.62	31	2.6	9.3	9.2	0.21	0.58	0.02	0.13	0.04	0.05	0.43	0.03
1.8	2.53	633	160	109.2	673	43796	21	22	48	55	14	0.08	152	0.91	1.28	40	0.6	27.6	13.9	0.12	0.15	0.47	0.03	0.06	0.07	0.60	0.01
3.1	1.96	332	88	35.4	621	34396	8	9	36	64	12	0.06	1014	0.60	0.36	44	0.3	35.5	21.2	0.11	0.00	0.81	0.02	0.10	0.06	0.29	0.01
4.3	2.47	838	215	77.9	1094	59365	20	30	50	160	15	0.09	852	0.64	0.52	88	0.8	47.2	16.3	0.06	0.00	0.01	0.03	0.24	0.10	0.37	0.01
5.5	0.41	62	8	6.7	116	34848	7	25	20	58	3	0.04	72	0.64	0.51	12	6.4	10.3	8.2	0.05	0.00	0.03	0.03	0.30	0.02	0.26	0.23
6.7	1.02	531	66	34.2	292	34264	7	14	51	144	9	0.08	368	0.39	0.30	123	1.1	15.7	14.0	0.14	0.31	0.00	0.02	0.09	0.03	0.65	0.02
8.2	0.88	138	45	18.1	444	25501	4	11	7	181	9	0.04	170	0.52	0.23	27	2.4	21.8	16.1	0.03	0.06	0.02	0.02	0.41	0.05	0.11	0.00
9.8	0.43	17	62	9.9	1883	40494	29	11	64	105	7	0.05	193	0.67	0.19	16	5.1	28.8	7.7	0.01	0.26	0.27	0.03	0.24	0.02	0.03	0.01
11.9	1.32	131	116	31.7	620	48508	18	19	51	129	9	0.12	1712	0.71	0.54	26	13.6	46.3	12.1	0.02	0.00	0.06	0.25	1.76	0.03	0.08	0.02
14.3	0.64	343	59	27.2	511	28994	14	11	84	153	7	0.04	206	0.34	0.25	50	6.4	9.6	13.4	0.13	0.16	0.03	0.07	0.19	0.03	0.12	0.01
16.5	1.87	530	115	46.9	671	36045	27	23	41	90	9	0.06	128	0.31	0.25	58	5.2	14.5	13.5	0.11	0.31	0.03	0.03	0.14	0.04	0.29	0.01
23.2	1.11	431	102	50.9	208	50735	23	50	118	64	11	0.08	89	0.92	0.39	38	3.4	8.7	5.6	0.17	0.49	0.03	0.16	0.05	0.04	0.51	0.03

Table 1 continued. ICP-MS results for elemental concentrations using EPA extraction method 3010A. Concentrations are reported as ppm (mg/kg). Solid line marks samples from above and below the saprolite/bedrock contact.

Core 1

Depth (m)	Te	I	Cs	Ba	La	Ce	Pr	Nd	Sm	Eu	Gd	Tb	Dy	Ho	Er	Tm	Yb	Lu	Hf	Ta	W	Hg	Tl	Pb	Bi	Th	U
0.6	0.03	0.53	9.2	508	66.6	16.3	16.0	62.0	12.8	3.0	13.5	2.0	11.3	2.1	5.7	0.8	4.9	0.7	0.7	0.02	0.08	0.00	0.85	12.8	0.19	6.65	0.70
1.8	0.03	0.28	8.4	212	43.4	41.6	11.3	45.0	9.5	2.1	10.0	1.5	8.2	1.5	4.2	0.6	3.8	0.6	0.9	0.02	0.09	0.01	1.02	16.8	0.37	6.90	1.57
3.1	0.05	0.16	8.1	255	31.5	31.9	8.3	34.1	6.9	1.6	7.2	1.0	5.7	1.0	2.9	0.4	2.6	0.4	0.6	0.01	1.32	0.03	0.80	21.9	0.37	8.27	1.39
4.3	0.01	0.23	4.7	526	54.4	105.6	14.7	61.6	12.5	2.7	12.2	1.6	8.6	1.6	4.3	0.6	3.7	0.6	0.7	0.02	0.10	0.03	0.90	29.5	0.24	7.26	0.00
5.8	0.02	0.27	5.2	543	24.9	32.0	6.9	29.3	6.1	1.6	6.1	0.9	4.8	0.9	2.5	0.3	2.1	0.3	0.6	0.01	0.08	0.01	0.82	8.2	0.15	6.94	0.61
7.6	0.03	0.06	4.0	148	40.1	82.2	10.7	43.3	8.4	1.7	8.1	1.1	5.0	0.8	1.9	0.3	1.7	0.3	0.6	0.01	0.06	0.00	1.11	8.9	0.37	6.56	1.60
8.5	0.06	0.03	4.4	311	14.0	33.1	4.3	17.5	3.6	0.7	3.6	0.5	2.8	0.5	1.5	0.2	1.4	0.2	0.8	0.01	0.05	0.01	0.64	13.7	0.35	8.41	0.00
10.1	0.04	0.08	4.3	297	13.9	37.4	4.8	19.5	4.2	1.0	3.9	0.6	3.4	0.7	1.8	0.3	1.8	0.3	0.6	0.01	0.06	0.03	0.68	17.6	0.19	11.28	2.19
11.6	0.04	0.04	5.9	500	32.1	75.3	9.0	36.3	7.7	1.3	6.9	0.8	3.8	0.6	1.4	0.2	1.1	0.2	0.5	0.01	0.14	0.02	0.78	14.4	0.36	5.90	0.00
13.7	0.05	0.07	10.6	444	174.8	320.4	34.1	138.7	27.6	4.7	27.2	2.9	11.3	1.7	4.0	0.5	3.3	0.5	0.5	0.02	1.31	0.03	0.52	75.0	0.54	5.48	3.65
15.3	0.04	0.04	5.7	264	76.4	137.7	15.5	63.2	12.1	2.3	11.8	1.5	6.2	0.9	2.0	0.2	1.4	0.2	0.4	0.01	0.40	0.03	0.73	20.1	0.75	9.04	0.00
19.2	0.09	0.01	4.0	165	51.3	114.3	13.7	55.2	10.6	2.1	10.1	1.2	5.3	0.7	1.5	0.2	0.9	0.1	0.3	0.01	2.21	0.02	0.63	9.9	1.09	10.93	2.84
20.7	0.16	0.00	4.2	240	15.2	34.3	4.2	16.8	3.4	0.7	3.2	0.4	2.2	0.3	0.8	0.1	0.5	0.1	0.4	0.01	0.12	0.04	0.76	9.1	1.81	11.23	2.61
21.4	0.00	0.01	4.9	26	62.4	133.9	16.1	67.3	13.5	2.8	13.6	1.7	6.6	0.9	1.8	0.2	1.3	0.2	0.5	0.00	5.09	0.27	0.65	20.7	0.60	43.78	1.40
21.8	0.01	0.00	18.2	50	2218.8	4963.0	589.4	2307.9	348.7	68.5	322.1	36.0	137.8	18.3	37.4	4.1	25.4	3.0	1.2	0.13	0.30	0.13	0.58	18.6	0.17	37.79	15.70

Core 2

Depth (m)	Te	I	Cs	Ba	La	Ce	Pr	Nd	Sm	Eu	Gd	Tb	Dy	Ho	Er	Tm	Yb	Lu	Hf	Ta	W	Hg	Tl	Pb	Bi	Th	U
0.6	0.03	0.42	1.9	87	10.4	36.0	3.0	12.7	2.8	0.6	3.3	0.5	2.6	0.5	1.3	0.2	1.0	0.1	0.4	0.01	0.34	0.02	0.50	16.0	0.34	8.90	1.16
1.8	0.04	1.24	3.0	255	40.3	69.4	12.6	53.7	11.1	2.4	10.0	1.4	7.8	1.5	4.0	0.6	3.8	0.5	0.7	0.02	0.69	0.16	0.46	34.0	0.25	12.74	1.41
3.1	0.34	0.94	2.1	243	40.2	41.1	10.8	43.9	9.9	2.2	10.5	1.6	9.6	1.8	5.3	0.8	4.9	0.7	1.0	0.01	0.09	0.01	0.34	28.3	0.78	9.58	1.75
4.3	0.05	0.80	4.6	388	45.0	44.3	12.3	51.6	11.8	2.9	12.9	2.1	12.7	2.4	6.8	0.9	6.0	0.9	0.7	0.02	0.18	0.02	0.61	33.3	0.57	8.57	1.84
5.5	0.01	0.06	1.2	50	18.6	35.3	5.1	20.9	4.5	0.9	4.5	0.6	3.0	0.5	1.3	0.2	1.1	0.2	0.3	0.01	0.92	0.03	0.15	10.0	0.15	8.10	0.00
6.7	0.10	0.16	6.0	203	21.5	21.3	6.1	26.0	5.7	1.2	5.3	0.8	4.5	0.8	2.3	0.3	2.0	0.3	0.6	0.01	0.11	0.02	0.66	22.7	0.47	8.49	1.89
8.2	0.02	0.10	0.9	120	28.9	28.8	7.9	33.0	7.1	1.5	7.2	1.1	6.3	1.2	3.1	0.4	2.6	0.4	0.7	0.01	0.05	0.02	0.16	65.6	0.45	6.21	3.35
9.8	0.05	0.23	0.7	156	39.4	163.6	10.1	40.1	8.0	1.9	8.9	1.3	7.7	1.4	3.8	0.5	3.1	0.4	0.3	0.01	0.34	0.03	0.49	56.3	0.26	6.59	2.80
11.9	0.09	0.08	1.2	267	108.8	162.8	27.5	106.5	21.5	4.0	19.2	2.7	14.6	2.6	6.8	0.9	5.5	0.7	0.6	0.03	0.08	0.02	0.14	60.3	0.82	7.12	3.71
14.3	0.03	0.02	2.1	302	10.7	29.2	3.6	15.6	3.6	0.7	3.6	0.5	3.0	0.6	1.5	0.2	1.3	0.2	0.6	0.01	0.04	0.00	0.32	28.0	0.27	8.46	1.70
16.5	0.00	0.01	4.5	452	29.4	70.0	8.6	36.1	7.8	1.4	7.4	1.0	5.1	0.8	2.0	0.3	1.5	0.2	0.7	0.01	0.51	0.02	0.45	8.0	0.16	7.71	1.27
23.2	0.04	0.00	2.2	105	10.9	24.4	3.0	12.3	2.7	0.6	3.1	0.4	2.6	0.4	1.1	0.1	0.8	0.1	0.2	0.00	0.16	0.02	0.64	6.7	0.29	9.48	1.17

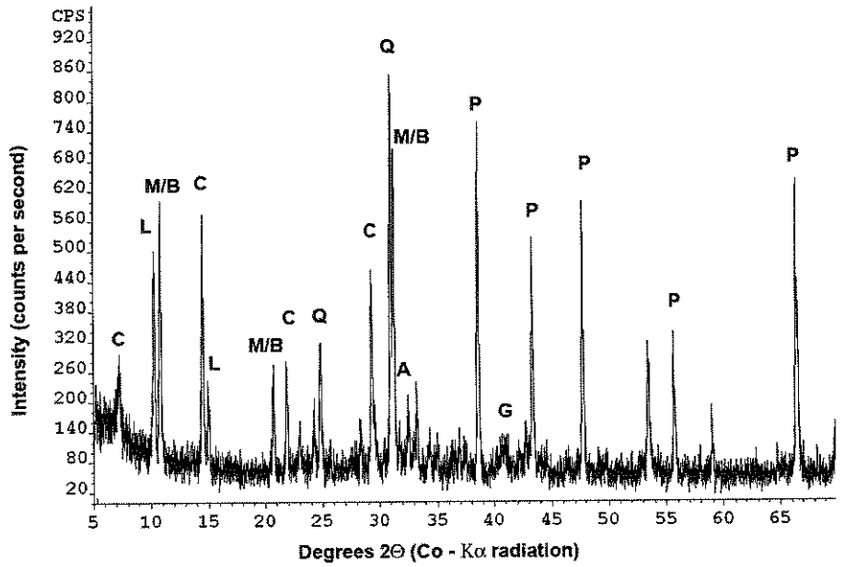

Figure 4. X-ray powder diffractogram of schist from core #2 (depth 21.8 m). Major minerals detected in pattern are noted by letters placed near strong reflections (Q) quartz, (B) biotite, (M) muscovite, (G) garnet, (C) clinochlore, (A) albite, (L) laumontite, and (P) pyrite.

As WDS maps of the same area seen in BSE (Figures 3C and 3D) show bands that trend with the foliation. The band in Figures 3B and 3C upper field of view highlights a concentration of pyrite (top). The band in Figures 3B, 3C, and 3D bottom field of view highlights arsenopyrite. The arsenopyrite blebs (Figure 3B inset) follow foliations, while pyrite continuously occurs in both foliations and in fractures.

Certain metals (e.g., Co, Ni, Mn, Cu, Pb, Zn) are known to isomorphously substitute into arsenopyrite structures (Wuensch, 1974; Morimoto and Clark, 1961). Some of these metals were detected by ICP-MS in the extractions (Table 1), however they were not specifically measured on the grains using WDS. It is possible these elements are present in the arsenopyrite structure but only As and Se were measured for the focus of this study. Analysis of nine different pyrite and arsenopyrite grains each, using WDS, reveals the following average percent concentrations and standard deviations: Pyrite Fe: 46.51 +/- 0.25, S: 53.49 +/-0.25, As: 0.00 +/- 0.00, Se: 0.00 +/- 0.00; Asenopyrite Fe: 33.21+/ -0.45, S: 20.54 +/-0.84, As: 46.15 +/-1.12, Se: 0.10 +/-0.01. Assuming Fe, As, S, and Se occur in their reduced states, these compositions yield structural formulae of $Fe_{0.998}S_2$ and $Fe_{0.938}As_{0.962}Se_{0.002}S_{0.998}$ for pyrite and arsenopyrite, respectively.

Saprolite and soil mineralogy are typical of the region, with soils being classified as Pacolet sandy loams (Tate, 1967). Optical examination of hand samples recovered from near the surface reveals the remnants of (Fe-rich) garnet and biotite. Their hydrolysis and oxidation products hematite (Fe_2O_3) and manganite (MnOOH) stain portions of the schist-saprolite red (Munsell 10R 5/4) and dark brown (10R 2.5/1), respectively. Also observed are goethite stains that appear as yellowish brown (7.5YR 5/6) in fractures. Goethite is a common hydrolysis product generated from oxidation of ferrous minerals, such as garnet, biotite, and pyrite (FeS_2), under slightly acidic conditions. Fine-grained sulfides are not observed in saprolite, however it is not uncommon to find pseudomorphic casts. Trace abundances of isometric casts can be found in the saprolite. The presence of these casts is consistent with pyrite being a trace component of the parent rock of the saprolite.

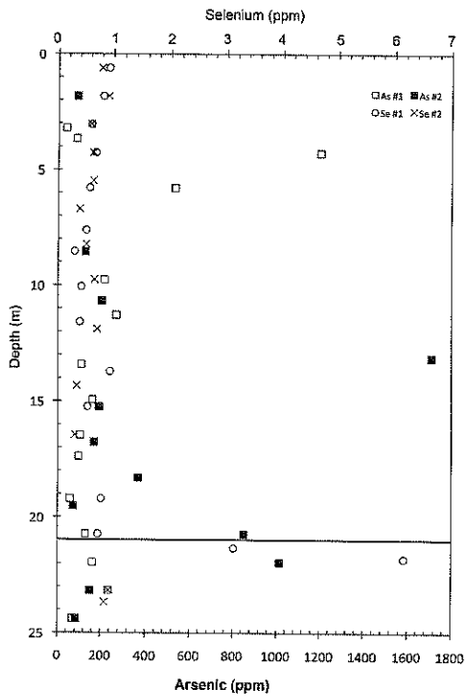

Figure 5. Arsenic and selenium concentrations of soil and rock samples of two core samples from Gwinnett County, GA. Concentrations are in ppm (mg per kg^{-1}) based on extractions using EPA method 3050A (Edgell, 1988) and subsequent measurement by ICP-MS (Hassan and Loux, 1990). Horizontal line at ~21m depth is approximate bedrock-saprolite boundary. Legend on upper right portion of graph shows respective symbols for arsenic (lower scale) and selenium (upper scale).

DISCUSSION

The large saprolite thickness of the study site and retrieval of the underlying bedrock allows for a meaningful context to evaluate natural versus anthropogenic origins of the high As values measured during the initial phase of the study as well as the co-existing Se in the arsenopyrite. Figure 5 shows a plot of As and Se concentrations versus depth in the two profiles. The first noticeable trend is the highly variable As concentrations that persist through both cores, with many values one to two orders of magnitude greater than the regional baseline value of 7 ppm. Arsenic values in the saprolite exceed those in the bedrock. In contrast the Se values are much higher in the bedrock when compared to the saprolite. In part, some of the variability can be attributed to compositional inhomogeneities of the schist as the evidence for moderately dipping foliations seen in the bedrock core and regional studies by Higgins and Crawford (2007). If a simplified assumption is made about the maximum availability of As and Se in the saprolite potentially coming from Brevard Zone bedrock, then the relative mobility of these two elements can be assessed for weathering conditions in this region of the Piedmont in the SE United States.

Model bedrock As and Se concentrations can be derived using the arsenopyrite stoichiometry measured in this study, assuming its volume abundance of 0.1% in the schist (Figure 3B), and densities of 2.7 and 6.2 g/cm^3 for the schist and arsenopyrite, respectively. These estimates result in bedrock concentrations of 1055 ppm for As and 23 ppm for Se and a relative As/Se for the bedrock of about 46. The measured ICP-MS values for the bedrock are somewhat lower with the greatest values being 75 ppm for As and 4 ppm for Se. These lower values can be attributed to incomplete extraction from the bedrock (see methods section) and inaccurate estimates in the model assumptions. The relative measured As/Se ratio is about 19, which is similar to regional values (Shacklette and Boerngen, 1984) and slightly less than the model estimate above. In contrast, the highest ICP-MS saprolite concentrations are 1396 ppm for As and 0.7 ppm for Se, which result in an As/Se ratio of 1990. The saprolite As value is very similar to the bedrock As value, even with correction for density differences due to silicate mass loss from hydrolysis. Most notable is the much lower value of Se in the saprolite, which is an order of magnitude less than the bedrock. The As/Se ratio is also notably orders of magnitude larger in the saprolite. This observation supports two important aspects regarding the fate and transport of As and Se in Piedmont weathered environments of the SE United States. Firstly, As appears to be relatively conserved during weathering and secondly, Se ap-

pears to be mobile and subject to transport away from the weathering zone.

The behavior of naturally occurring As in arsenopyrite and its oxidized forms can be understood in terms of location within the bedrock/saprolite/soil profile and available electron acceptors in the weathering profile. The oxidation from $As^{(III)}$ in arsenopyrite to $As^{(V)}$ is a well-studied process with associations to microbially mediated lithotrophy during weathering (Ehrlich, 1964; Strawn and others, 2002; Yu Yunmei and others, 2004). An important consequence of this oxidation reaction is the generation of acidity and the production of arsenate complexes (Walker and others, 2005). The latter of which behave much like soil phosphate complexes that are know to associate with Fe-oxide surfaces. (Qafoku and others, 1999; Filippi and others, 2007; Neel and others, 2003). Given the abundance of hematite and goethite in these piedmont soils, the retention of As relative to bedrock concentrations in this study can be parsimoniously explained as a natural occurrence related to the original bedrock. The heterogeneous vertical distribution As and its concordance of mass balance between bedrock and weathered horizons are in contrast to known studies of anthropogenic As occurrences. For example, Kukier and others (2001) amended similar Georgia Piedmont Cecil soils with As-bearing fly ash. In this anthropogenic case, a signature distribution of As is characterized by a high near the surface followed by a gradational decrease at depth to an order of magnitude lower level.

The behavior of naturally occurring Se, as it is released during arsenopyrite oxidation, is not as well documented as As. Se in arsenopyrite most likely occupies sulfur sites in arsenopyrite as a reduced selenide form. Upon exposure to electron acceptors such as oxygenated ground waters, the Se reacts to form the oxidized states of $Se^{(IV)}$ and $Se^{(VI)}$, with the latter selenate form being more common in weathering environments (Strawn and others, 2002). Comparison of As and Se ionic potentials [IP = defined as the ratio of ionic charge (Z) to ionic radius (r)] predicts their solubility behavior to be different (Pauling, 1948). Assuming the respective values of $r_{As(V)} = 0.46$Å and $r_{Se(VI)} = 0.42$, then respectively $IP_{As(V)} = 10.9$ and $IP_{Se(VI)} = 14.2$. These IP values indicate that both As and Se should complex as soluble radicals. The greater IP value of $Se^{(VI)}$ indicates it is more soluble than As, which is consistent with the observations of this study. Studies of both As and Se for the Georgia Piedmont are not extensive, however Peltier and others (2008) have indirectly evaluated heavy metal abundance in watersheds by using the Asiatic clam (*Corbicula fluminea*) as a biomonitor. The studies specific interest is the contributions of trace elements associated with different point sources and land uses in a large river. In particular they studied the tributaries of the Chattahoochee River, whose main channel in the Georgia Piedmont is largely controlled by the trace of the Brevard Zone. Realizing that the Chattahoochee integrates a watershed larger than the Brevard Zone, analysis of As and Se in nine samples from each of fifteen river sites reveals an As/Se ratio of 0.6, which is much smaller than the ratios of about ~40 for the bedrock and ~2000 for the saprolite at the study site. If the primary As and Se signature of the Georgia Piedmont is controlled by arsenopyrite similar to that in this study area, then both the saprolite and the river waters (as proxied by a biomonitor of Peltier and others, (2008)) provide a good model for the partitioning of the two elements in the Piedmont of SE United States.

CONCLUSIONS

Pyrite and arsenopyrite occur in a mafic schist of the Piedmont of Gwinnett County, Georgia associated with a fossil hydrothermal system and the Brevard Zone. The pyrite is texturally associated with late stage retrograde metamorphic laumontite, which occurs along brittle fractures and within foliations. Arsenopyrite appears as discreet grains within and associated with foliations formed or retained during prograde metamorphism. Analysis of the As and Se in the bedrock shows they reside in the arsenopyrite resulting in bulk rock concentrations above regional baseline values. Analysis of the As and Se in overlying saprolite and

soil indicates they are weathered from the arsenopyrite but have different fates. Arsenic is conserved most likely as arsenate complexes adsorbed to abundant Fe-oxyhydroxide surfaces in the saprolite/soil. Selenium is transported out of the weathering profile and presumed to be carried off by the rivers. This scenario is directly supported by the high As/Se ratios measured in the saprolite of this study and indirectly by the very low As/Se ratios measured in biomonitor proxies of river waters draining the Brevard Zone (Peltier and others, 2008). Ascribing high concentrations of As and Se to anthropogenic, natural, or false-positive factors requires analysis of bedrock, saprolite, soil, and methodology (in aluminous terrains). In cases where As concentrations are high at the surface and decrease to regional baseline values, then an anthropogenic cause might be ascribed. In the case of this study, where there are no discrete vertical trends and mass balancing of underlying bedrock can account for saprolite concentrations, naturally elevated As levels are possible on small spatial scales in the Piedmont soils of the SE United States.

ACKNOWLEDGEMENTS

The author is indebted to Chris Fleisher (EMPA) and Sayed Hassan (ICP-MS) for their expert skills and friendly demeanors. Thanks are given to the University of Georgia Departments of Geology and Crop and Sciences for access to their analytical facilities. The review of David Leigh significantly improved the manuscript.

REFERENCES

Bednar, A.J., Garbarino, J.R., Ranville, J.F. and Wildeman, T.R., 2002. Presence of Organoarsenicals Used in Cotton Production in Agricultural Water and Soil of the Southern United States. Journal of Agricultural and Food Chemistry, 50(25): 7340-7344.

Crawford, T.J. and Kath,.R.L., 2001. The Brevard Zone: A literature Review. In: T.J. Kath R. L. and Crawford (Editor), Across the Brevard Zone: The Chattahoochee Tunnel, Cobb County, Georgia. Georgia Geological Society Guidebooks, pp. 1-16.

Deer, W.A., Howie, R.A., Wise, W.S. and Zussman, J., 2004. Rock-forming minerals: Framework Silicates, Volume 4B. Geological Society, London, 982 pp.

Dicken, C.L., Nicholson, Suzanne W., Horton, John D., Foose, Michael P. and Mueller, Julia A.L., 2005. Preliminary integrated geologic map databases for the United States. U.S. Geological Survey, pp. 44.

Edgell, K., 1988. USEPA method study 37-SW-846 method 3050 acid digestion of sediments, sludges and soils. In: E.C. 68-03-3254. (Editor), pp. 12.

Ehrlich, H.L., 1964. Bacterial oxidation of arsenopyrite and enargite. Economic Geology, 59(7): 1306-1312.

EPA Report 2003, U.S. EPA Workshop on Managing Arsenic Risks to the Environment: Characterization of Waste, Chemistry, and Treatment and Disposal, EPA/625/R-03/010: Denver, Colorado, National Risk Management Research Laboratory Office of Research and Development U.S. Environmental Protection Agency, Cincinnati, OH 45268, 107 pp.

Filippi, M., Dousova, B. and Machovic, V., 2007. Mineralogical speciation of arsenic in soils above the Mokrsko-west gold deposit, Czech Republic. Geoderma, 139(1-2): 154-170.

Frankenberger, W.T., 2002. Environmental chemistry of arsenic. Books in soils, plants, and the environment. Marcel Dekker, New York, xiii, 391 pp.

Haney, P.B., W.J. Lewis, and W.R. Lambert. 2009. Cotton production and the boll weevil in Georgia: History, cost of control, and benefits of eradication. Univ. of Georgia Agric. Exp. Stn. Research Bulletin 428, 34 pp.

Hassan, S.M. and Loux, N.T., 1990. Elimination of spectral interference in inductively coupled plasma atomic emission spectroscopy using orthogonal ploynomials. Spectrochemica Acta, 45B: 719 - 729.

Higgins, M.W., 1966. Geology of the Brevard Lineament near Atlanta. In: M. Georgia Department of Mines, and Geology. Geological Survey Bulletin 77, Atlanta, GA, 49 pp.

Higgins, M.W. 1968. Geologic map of the Brevard fault zone near Atlanta, Georgia, Miscellaneous geologic investigations map I-511. U.S. Geological Survey, Washington, D.C.

Higgins, M.W. and.Crawford, Ralph F., 2007. Geologic Map of the Atlanta 30' x 60' Quadrangle, GA. Version 4.1.0. Geologic Mapping Institute and Atlanta Geological Society, Clayton, GA.

Jackson, B.P. 1998. Trace element solubility from land application of fly ash/organic waste mixtures with emphasis on arsenic and selenium speciation. Thesis (PhD), University of Georgia, 151 pp.

Jones, C.L., Hodge, V. F., Schoengold, D. M., Biesiada H., and Starks, T. H., 1987. An Interlaboratory Study of Inductively Coupled Plasma Atomic Emission Spectroscopy Method 6010 and Method 3050. In: U.S. Environmental Protection Agency (Editor), Las Vegas. Nevada., 34 pp.

Kukier, U., Sumner, M.E. and Miller, W.P., 2001. Distribution of exchangeable cations and trace elements in the profiles of soils amended with coal combustion by-products. Soil science, 166(9): 585-597.

Morimoto, N. and Clark, L.A., 1961. Arsenopyrite crystal-chemical relations. American Mineralogist, 46(11-12): 1448-1469.

Neel, C., Bril, H., Courtin-Nomade, A. and Dutreuil, J.P., 2003. Factors affecting natural development of soil on 35-year-old sulphide-rich mine tailings. Geoderma, 111(1-2): 1-20.

Pauling, L., 1948. The nature of the chemical bond, and the structure of molecules and crystals: An introduction to modern structural chemistry. H. Milford, Oxford University Press, Ithaca, N.Y. London, 450 pp.

Peltier, G.L., Meyer, J.L., Jagoe, C.H. and Hopkins, W.A., 2008. Using trace element concentrations in Corbicula fluminea to identify potential sources of contamination in an urban river. Environmental Pollution, 154(2): 283- 290.

Qafoku, N.P., Kukier, U., Sumner, M.E., Miller, W.P. and Radcliffe, D.E., 1999. Arsenate displacement from fly ash in amended soils. Water, air, and soil pollution, 114(1/2): 185-198.

Reed, J.C., 1970. The Brevard Zone: A re-interpretation. In: G.W. Fisher, Pettijohn, F.J., Reed, J.C. Jr., and Weaver, K.N. (Editors), Studies of Appalachian geology: central and southern. Interscience Publishers, New York, pp. 261-269.

Shacklette, H.T., and Boerngen, J.G., 1984. Element concentrations in soils and other surficial materials of the conterminous United States, U.S. Geological Survey Professional Paper 1270. Professional Paper, 105 pp.

Strawn, D., Doner, H., Zavarin, M. and McHugo, S., 2002. Microscale investigation into the geochemistry of arsenic, selenium, and iron in soil developed in pyritic shale materials. Geoderma, 108(3-4): 237-257.

Tate, R.J., 1967. Soil Survey, Gwinnett County, Georgia. In: U.S. Department of Agriculture, Washington, DC.

Walker, S.R., Jamieson, H.E., Lanzirotti, A., Andrade, C.F. and Hall, G.E.M., 2005. The Speciation Of Arsenic In Iron Oxides In Mine Wastes From The Giant Gold Mine, N.W.T.: Application Of Synchrotron Micro-Xrd And Micro-Xanes At The Grain Scale. Canadian Mineralogist, 43(4): 1205-1224.

Williams, P.N. and others, 2005. Variation in Arsenic Speciation and Concentration in Paddy Rice Related to Dietary Exposure. Environmental Science & Technology, 39(15): 5531-5540.

Wuensch, B.J., 1974. Sulfide crystal chemistry. Mineralogical Society of America Short Course Notes, 1: 24.

Yu Yunmei, Zhu Yongxuan, Williams-Jones, A.E., Gao Zhenmin and Li Dexian, 2004. A kinetic study of the oxidation of arsenopyrite in acidic solutions; implications for the environment. Applied Geochemistry, 19(3): 435-444.